Experimental observation of the structure of gaskinetic magnetic resonance

V. S. Laz'ko

I. V. Kurchatov Institute of Atomic Energy

It was observed in experiment, with N_2 and CO as examples, that resonant decrease of thermal conductivity of gases in mutually perpendicular dc and ac magnetic fields (gaskinetic magnetic resonance—GMR) has a structure in the form of resonant peaks of the thermal conductivity at ac frequencies that are multiples of its fundamental frequency. The results are in qualitative agreement with the theory. It is shown that the concrete form of the structure is theoretically determined by the chosen model of the angular dependence of the molecule-scattering probability. A discrepancy with the experimental data was observed for the customary model, in which the scattering cross section is determined by second-order Legendre polynomials of the angles between the velocity and momentum vectors of the colliding molecules. This points to flaws in the model. A possible physical interpretation of the observed phenomenon is briefly expounded.

It was shown theoretically in Refs. 1 and 2 that in mutually perpendicular (crossed) dc (**H**) and ac (**H**$_{\sim}$) magnetic fields the thermal conductivity of a gas undergoes, in addition to the decrease $\Delta\varkappa_s$ due to the field **H** [the Senftleben-Beenaker effect (SBE)[3–6]] an additional resonant decrease $\Delta\varkappa_+$. The latter reaches the resonant value at $\omega_r = \gamma H_r$, where H_r and ω_r are the resonant values of the field H and of the frequency ω of the field $H_{\sim}$, while γ is the rotational gyromagnetic ratio of the gas molecules (gaskinetic magnetic resonance—GMR). In Ref. 2, in addition, a GMR structure was predicted in the form of resonant changes of the thermal conductivity at frequencies ω that are multiples of ω_r (GMR harmonics[1]). The GMR was observed experimentally and investigated in the gases O_2, N_2 and CO.[7–9] In this paper experiments aimed at observing and investigating the GMR structure in N_2 and CO are described.

A schematic diagram of the measurements is shown in Fig. 1. The temperature-sensitive resistors of two identical heat-conduction sensors, similar to those described in Ref. 10, were connected in adjacent arms of a Wheatstone bridge fed from a storage-battery bank. The sensors were placed in a common dc magnetic field H. One of the sensors (active, S_a) was inside the high-frequency solenoid L that produced an ac field $H_{\sim} = 2H_1\sin\omega t$ perpendicular to **H**.

The second (comparison, S_c) sensor is shielded against the field $H_{\sim}$ and serves to cancel the bridge unbalance due to the SBE in the field H. In addition, the presence of the sensor S_c lowers the thermal drift of the unbalance. All experiments, with a rare exception (see below), were carried out
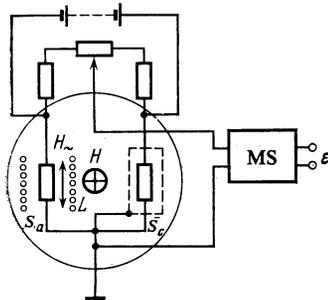
with the apparatus and procedure described in detail in Ref. 9. A modulation method of measurement was used, similar to that employed in Ref. 8. It consisted of the following. A modulating field $h\|H$ whose value is changed jumpwise from $h = 0$ to $h = h(t)$ and back to zero, with a period $T = 4$ sec is superimposed on a dc field of prescribed value H_0. The value of $h(t)$ increases linearly with the time t at a chosen rate. As a result, the thermal conductivity of the gas in the sensors varies periodically between $\varkappa(H_0)$ and $\varkappa[H_0 + h(t)]$. The ensuing changes of the bridge unbalance are amplified and synchronously detected by the measuring system (MS), see Fig. 1. The output signal ε of this system is proportional to the change of the thermal conductivity

$$\Delta\varkappa = \varkappa(H_0 + h(t)) - \varkappa(H_0)$$

of the gas in the sensor S_a (i.e., in the crossed fields), after subtracting the change of the thermal conductivity

$$\Delta\varkappa_s = \varkappa_s(H_0 + h(t)) - \varkappa_s(H_0)$$

in the sensor S_c (i.e., produced in the constant SBE field)

$$\varepsilon \infty \Delta\varkappa - \Delta\varkappa_s = \Delta\varkappa_+.$$

Variation of $h(t)$ from $h(0) = 0$ to $h(t_{max}) = h_{max}$ sweeps the quantity $\Delta\varkappa_+$ over H from H_0 to $H_0 + h_{max}$. Usually $t_{max} \approx 30$ min and $h_{max} \approx 300$ Oe. The signal ε was recorded with an automatic plotter. The experiments performed with $H, H_1, f = \omega/2\pi$ and pressure p in the ranges 0–25 kOe, 60–180 Oe, 183–606 kHz and 7–60 mTorr.

Figure 2 shows by way of example typical $\Delta\varkappa_+(H)$ plots for two orientations of the temperature gradient. $\nabla T \| H$ and $\nabla T \perp H$. The ordinate axis is directed towards decreasing $\Delta\varkappa_+$. Minima of the known GMR effect are seen at $H = H_r$, and at $H = H_m$ one can see maxima of $\Delta\varkappa$ (marked by the arrow) with amplitude λ smaller by about an order of magnitude than that of the GMR. The value of H_m, as seen from the figure, does not depend of the direction of ∇T. The rise of the curves at small H is due to the differential SBE as a result of the insufficient (in this example) compensation of the SBE by the sensor S_c. It was established in the experiments that if δ of the differential SBE is small enough (usually $\delta \lesssim 10^{-2}$ $\Delta\varkappa_S$) its effect on H_m and λ can be neglected. The reason is that the value of the SBE at $H = H_m \gtrsim 0.7$ kOe and at a pressure p 30 mTorr is close to saturation, i.e., to the value as

FIG. 1. Schematic diagram of experimental setup.
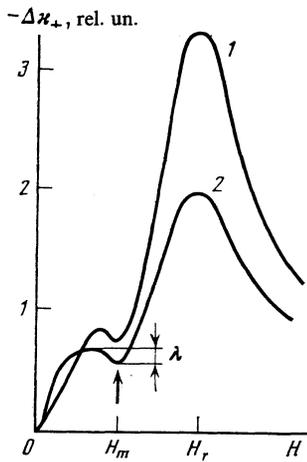
FIG. 2. Experimental plots of the change $\Delta\varkappa_+(H)$ of the thermal conductivity of CO gas in crossed fields. $H_1 = 180$ kOe, $f = 338$ kHz, and $H_r = 1660 \pm 30$ Oe, 1) $\nabla T \| \mathbf{H}$; 2) $\nabla T \perp \mathbf{H}$.

$H \to \infty$, therefore δ changes little when H changes by an amount of the order of the width of the maximum.

Figure 3 shows experimental plots of λ vs f, H_1, and p. To take into account the pressure dependence of the thermal conductivity, which is substantial at small p, the ordinate is graduated in $\lambda /S^{\|}$, where $S^{\|}$ is the SBE at saturation for the corresponding pressure and at $\nabla T \| \mathbf{H}$. It can be seen from Figs. 3a and 3b that $\lambda /S^{\|}$ increases with increasing H_1 and with decreasing f. At low p (see Fig. 3c) $\lambda /S^{\|}$ increases with increasing pressure, but at $p \gtrsim 20$ mTorr the dependence becomes weak. The experiments have shown that H_m changes in direct proportion to the frequency f. For N_2 and CO we have, accurate to $\lesssim 5\%$, $f/H_m = 2\gamma^* = 2\gamma/2\pi$, i.e., $H_m = H_r/2$ (according to Ref. 5 γ^* is equal $210 + 10$ and 195 ± 10 Hz/Oe for N_2 and CO, respectively). In other
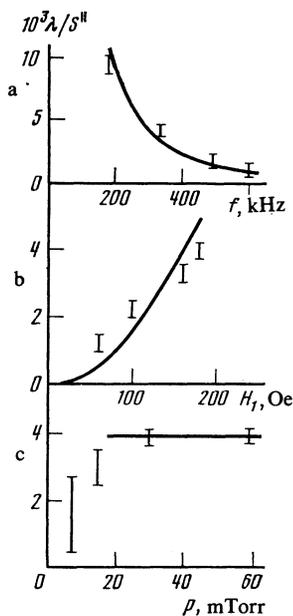
FIG. 3. Experimental plots for N_2 at $\nabla T \| \mathbf{H}$: a) of $\lambda /S^{\prime\prime}(f)$ at $H_1 = 180$ Oe and $p = 30$ mTorr; b) of $\lambda /S^{\prime\prime}(H_1)$ at $f = 338$ kHz and $p = 30$ mTorr; c) of $\lambda /S^{\prime\prime}(p)$ at $f = 338$ kHz and $H_1 = 180$ Oe. Solid curves—theoretical.
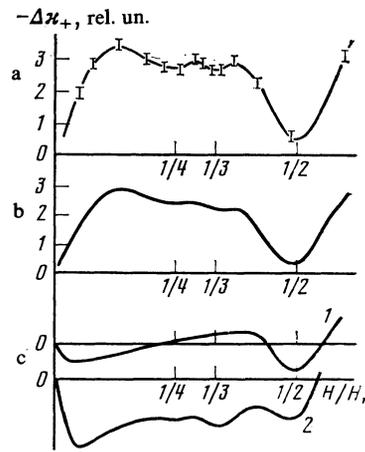
FIG. 4. Normalized experimental plots: $\Delta\varkappa_+(H/H_r)$, $p = 30$ mTorr: a) $f = 183$ kHz, $H_1 = 130$ Oe; b) $f = 338$ kHz, $H_1 = 180$ Oe; c) theoretical curves for the models (see the text) with: 1) $l_1 = 1$ and $l_2 = 2$; 2) $l_1 = 3$ and $l_2 = 4$.

words, at $H = H_m$ the field frequency ω is equal to double the GMR resonant frequency corresponding to H_m, i.e., $\omega = 2\gamma H_m = 2\omega_r$.

Figure 4 shows the results of the experiments performed with an aim at observing the harmonics at $\omega = k\omega_r$, where $k > 2$. The curve for $f = 183$ kHz was obtained by the "triple count" method,[11] whereas the curve for $f = 338$ kHz was obtained by the procedure described above. The mean squared error of the latter curve is within the thickness of the line. Harmonics corresponding to $k = 3$ and $k = 4$ are resolved on both curves.

In Ref. 2 the GMR harmonics were predicted for conditions when the frequency γH_1 is low compared with the characteristic relaxation frequency v. In the experiments described $\gamma H_1/v \sim 1$, we therefore turn to Ref. 1, in which expressions were obtained for the transport coefficient at arbitrary $\gamma H_1/v$. These expressions, with insignificant abbreviation and change of notation, can be rewritten in the form

$$\Delta\varkappa \propto - \sum_{m_1+m_2=m} (C^{1m}_{l_1 m_1 l_2 m_2})^2 \Delta a_{m_2}, \tag{1}$$

$$\Delta a_{m_2} = \sum_{q=-l_2}^{l_2} |D^{l_2}_{m_2 q}(\cos\theta)|^2 \frac{x^2_{m_2 q} + i v x_{m_2 q}}{v^2 + x_{m_2 q}^2}, \tag{2}$$

$$x_{m_2 q} = m_2\omega + q[(\gamma H - \omega)^2 + (\gamma H_1)^2]^{1/2}, \tag{3}$$

where C are Clebsch-Gordan coefficients, the indices l_1, m_1, l_2, and m_2 are determined by the chosen model of the angular dependence of the molecule scattering probability,

$$\cos\theta = (\gamma H - \omega)/[(\gamma H - \omega)^2 + (\gamma H_1)^2]^{1/2},$$

and the quantities $D(\cos\theta)$ are defined, e.g., in Ref. 12. Re$\Delta\varkappa$ corresponds to the change $\Delta\varkappa$ measured in the present experiments along ∇T, and Im$\Delta\varkappa$ corresponds to the so-called odd effect, i.e., to the onset of heat flow along the direction $\nabla T \times \mathbf{H}$. The terms in (1) with $m_2 = 0$ describe the known GMR effect, while at $m_2 \neq 0$ and $|\gamma H - \omega| \gg \gamma H_1$ we have

$$\cos\theta \approx 1, \quad D^{l_2}_{m_2 q} \approx \delta_{m_2 q}$$

(here δ_{m_2q} is the Kronecker delta), so that we get an Re$\Delta \varkappa(H)$ dependence close to that in the SBE. The small "off diagonal" terms, of order of $(H_1/H)^2$, in Eq. (2) with $m_2 \neq q$ describe the deviation from this dependence and have a non-monotonic character. Indeed when the ratios of ω and γH are such that $x_{m_2q} = 0$, terms with definite values of q vanish in the sum (2). If H_1/H is neglected, these relations take the simple form

$$\omega = \omega_{m_2q} = q\gamma H/(q \pm m_2)$$

and yield the frequencies ω_{m_2q} (or the constant fields H_{m_2q}), at which maxima of $\Delta \varkappa_+$ should be observed in accordance with (1). Since the subscripts m_2 and q are determined by the scattering model, the ω_{m_2q}, spectrum obtained from experiment can yield useful information for choosing an adequate model. Thus, expressions (1), (2), and (3) with index $l_2 = 2$ correspond to the so-called "P_2 model"[2,5,9] that describes well the transport coefficients in external fields. This model, however, is apparently only a good approximation, since it gives maxima of $\Delta \varkappa_+$ only if $k = 2$. Observation of maxima at $k > 2$ means that the more accurate model should contain $l_2 > 2$.

Figure 4c shows plots of $\Delta \varkappa_+(H)$ calculated for the models $l_1 = 1$, $l_2 = 2$ (the P_2 model) and $l_1 = 3$, $l_2 = 4$ for parameters close to those in the experiment, viz., $H_1 = 180$ Oe, $f = 340$ kHz, and $p = 30$ mTorr. It can be seen that, as in the experiment, the second model gives a maximum at $H/H_r = 1/3$ and $1/4$. It can be stated on this basis that to improve the P model it is necessary to add the terms with $l_1 = 3$ and $l_2 = 4$.

For comparison with the experimental dependence of λ on H_1, f, and p with the theory, we note that in experiment the quantities $\sin^2\theta$ and $v^2/[(\gamma H - \omega)^2 + (\gamma H_1)^2]$ are small ($\sim 10^{-2}$). Equation (1) in lowest order in $\sin^2\theta$ shows that λ as a function of H_1 and ω is given by $\lambda \propto (\gamma H_1/\omega^2)$, and its dependence on v is weak. We emphasize that this conclusion is not connected with the choice of the model and is general.

Comparison with experiment shows that at $p > 20$ mTorr (see Fig. 3c) the λ ($p \propto v$) dependence is indeed weak, and is enhanced at low pressures probably because of the stronger influence of the sensor walls, for even at $p = 15$ mTorr the Knudsen number is Kn $\approx 0.3 \sim 1$. The λ (f) dependence agrees well with the theory (see Fig. 3a). It can be seen from Fig. 3b that the increase of λ with increasing H_1 follows the theoretical tendency, but the λ (H_1) dependence deviates noticeably from quadratic. Exact determination of these dependences was not the aim of the present study and would require special measurements.

The occurrence of $\Delta \varkappa_+$ maxima at GMR frequencies can be attributed to distinctive features of the microscopic motion of rotating-top molecules in crossed field. The thermal conductivity decreases in the field because the scattering probability of polyatomic gas molecules depends on the directions of their torques M, and their precession in the field

during the free path time increases their collision probability by increasing the number of different orientations of M (the effective collision cross section is increased). The "increase of the number of orientations" means that when the field is turned on the share of phase space of the vector M of each molecule in the phase space of the orientation of M is increased by a definite amount $\Delta \Gamma$. Indeed, following Ref. 13, it is easy to show that as the unit vector $\mathbf{n} = \mathbf{M}/M$ moves in the crossed fields it traces on the unit sphere trajectories that do not leave the spherical strip of width

$$2\theta = 2 \arcsin (\gamma H_1 [(\gamma H - \omega)^2 + (\gamma H_1)^2]^{-1/2}).$$

It is this width which determines the value of $\Delta \Gamma$ when H, H_1, and ω are given. When $\omega = \gamma H$ and $\theta = \pi/2$ the width $\Delta \Gamma$ reaches its maximum limit and the thermal conductivity decreases resonantly (GMR). It follows from Ref. 13 that the trajectories of $\mathbf{n}$ are similar to Lissajous figures and become closed and stationary for all molecules (at constant γ) at $\omega = k\gamma H$, $k = 2, 3, 4, \ldots$ (neglecting the value of H_1/H). This decreases $\Delta \Gamma$ (which is now determined by the trajectory length) and should therefore result in a maximum of the thermal conductivity λ. In addition, it follows from the expression for θ that λ increases with increasing H_1 and with decreasing ω, in agreement with experiment.

In conclusion, the author thanks L. L. Gorelik, L. A. Maksimov, and A. A. Sazykin for helpful discussions of the results.

---

[1] As applied to GMR, this term was proposed by L. L. Gorelik and L. A. Maksimov.

---

[1] V. D. Borman, L. A. Maksimov, Yu. V. Mikhailov, and B. I. Nikolaev, Zh. Eksp. Teor. Fiz. **53**, 2143 (1967) [Sov. Phys. JETP **26**, 1210 (1968)].
[2] L. A. Maksimov, Kinetic Theory of Gases with Rotational Degrees of Freedom, Doctoral Dissertation, Moscow, 1971.
[3] H. Senftleben and J. Piezner, Ann. Phys. **16**, 907 (1933); **27**, 108 (1936); **30**, 541 (1937).
[4] L. L. Gorelik, Yu. M. Redkoborodyĭ, and V. V. Sinitsyn, Zh. Eksp. Teor. Fiz. **48**, 761 (1965) [Sov. Phys. JETP **21**, 503 (1965)].
[5] Yu. M. Kagan and L. A. Maksimov, ibid. **51**, 1893 (1966) [**24**, 1272 (1967)].
[6] J. F. Hermans, J. H. Koks, A. F. Hengeveld, and H. F. P. Knaap, Physica (Utrecht) **50**, 410 (1970).
[7] V. D. Borman, L. L. Gorelik, B. I. Nikolaev, and V. V. Sinitsyn, Pis'ma Zh. Eksp. Teor. Fiz. **6**, 945 (1967) [JETP Lett. **6**, 362 (1967)].
[8] V. D. Borman, L. L. Gorelik, V. S. Laz'ko, et al., Inst. Atom. Energy Preprint IAE-2623, 1976.
[9] L. L. Gorelik and V. S. Laz'ko, Zh. Eksp. Teor. Fiz. **84**, 931 (1983) [Sov. Phys. JETP **57**, 541 (1983)].
[10] V. D. Borman, L. L. Gorelik, V. S. Laz'ko, et al., Prib. Tekh. Eksp. No. 2, 232 (1975).
[11] V. D. Borman, L. L. Gorelik, B. I. Nikolaev, et al. Zh. Eksp. Teor. Fiz. **56**, 1788 (1969) [Sov. Phys. JETP **29**, 959 (1969)].
[12] E. M. Lifshitz and L. P. Pitaevskii, Relativistic Quantum Theory, Part 1, Pegamon, 1970.
[13] J. I. Rabi, N. F. Ramsey, and J. Schwinger, Rev. Mod. Phys. **16**, 176 (1954).

Translated by J. G. Adashko

460   Sov. Phys. JETP **60** (3), September 1984

V. S. Laz'ko   460